

INACTIVATION OF VOLTAGE-GATED Ca^{2+} CHANNELS AND CONE-ROD DYSTROPHY CORD7

Minoru Wakamori¹⁾, Yoshitsugu Uriu²⁾, Takafumi Miki²⁾,
Shigeki Kiyonaka²⁾ and Yasuo Mori²⁾

Abstract Active zones are highly specialized sites for release of neurotransmitter in presynaptic nerve terminals. The spacing between voltage-dependent calcium channels (VDCCs) and synaptic vesicles at active zones is thought to influence the dynamic properties of synaptic transmission. Recently we have demonstrated a novel molecular interaction between VDCCs and an active zone scaffolding protein, rab3-interacting molecule 1 (RIM1). The RIM1 induced a pronounced deceleration of inactivation rate and a depolarizing shift of the inactivation curve of recombinant P/Q-type VDCC expressed as $\alpha_{1A}\alpha_2/\delta\beta_{1a}$ complex in baby hamster kidney cells. During 2-s voltage-displacement to -30 mV, which is the threshold of the P/Q-type VDCC activation, almost all channels were inactivated in the absence of the RIM1 (closed-state inactivation), but less than 20% of the channels were inactivated in the presence of the RIM1. Thus, the RIM1 coordinates calcium signaling and spatial organization of molecular constituents at presynaptic active zone.

A mutation has been identified for an autosomal dominant cone-rod dystrophy CORD7 in the *RIM1* gene. Interestingly, the affected individuals showed significantly enhanced cognitive abilities across a range of domains. The mouse RIM1 arginine-to-histidine substitution (R655H), which corresponds to the human CORD7 mutation, modifies RIM1 function in regulating VDCC currents elicited by the P/Q-type Cav2.1 and L-type Cav1.4 channels. The data can raise an interesting possibility that CORD7 phenotypes including retinal deficits and enhanced cognition are at least partly due to altered regulation of presynaptic VDCC currents.

Hirosaki Med. J. 61, Supplement : S53—S62, 2010

Key words: Calcium channel; inactivation; neurotransmission; RIM; Cone-Rod Dystrophy

Voltage-gated Ca^{2+} channel

Voltage-gated calcium channels (VGCCs) or voltage-dependent Ca^{2+} channels (VDCCs) are ion channels that are expressed widely and mainly in excitable cells, and mediate Ca^{2+} influx in response to membrane depolarization. Because Ca^{2+} functions as a critical intracellular messenger, Ca^{2+} influxes not only depolarize the membrane potential but also regulate various intracellular processes¹⁾. VGCCs are involved directly and indirectly in a broad spectrum of cellular processes.

Multiple types of VDCCs are distinguished on the basis of biophysical and pharmacological properties²⁾. High voltage-activated types of VDCCs known for their essential involvement in neurotransmitter release are N-, P/Q-, R-, and L-types³⁻⁵⁾. Molecularly, it has been accepted that VDCCs are heteromultimeric protein complexes comprised of the pore-forming α_1 subunit, designated as Ca_v , and auxiliary subunits such as α_2/δ , β , and γ ³⁾. The α_1 subunit is encoded by at least 10 distinct genes, subdivided into three major families, Ca_v1 (L type), Ca_v2 (N, P/Q and R type), and Ca_v3 (T type), whose correspondence

¹⁾Department of Oral Biology, Tohoku University Graduate School of Dentistry, Sendai 980-8575, Japan, ²⁾Department of Synthetic Chemistry and Biological Chemistry, Kyoto University Graduate School of Engineering, Kyoto 615-8510, Japan
Correspondence: Minoru Wakamori, Ph.D.
Laboratory of Molecular Pharmacology & Cell

Biophysics, Department of Oral Biology, Tohoku University Graduate School of Dentistry, Sendai 980-8575, Japan
Phone: 022-717-8310
Facsimile: 022-717-8313
E-mail: wakamori@m.tains.tohoku.ac.jp

with functional types is largely elucidated^{2,6}. The cytoplasmic β subunit interacts with the α_1 subunit to enhance functional channel expression through trafficking to the plasma membrane^{7,8}. The β subunits dramatically modulate multiple gating parameters in activation and inactivation processes^{9,12}.

Reduction of distance between synaptic vesicles and VDCCs by RIM1

The active zone is the specific site for action potential dependent exocytosis of neurotransmitters at synapses of the nervous system across species^{13,14}. The molecular organization of active zones, where synaptic vesicles are docked in the close vicinity of VDCCs at the presynaptic membrane, is essential for the control of neurotransmitter release triggered by depolarization-induced Ca^{2+} influx. The spacing between VDCCs and vesicles at active zone is particularly thought to influence the dynamic properties of synaptic transmission¹⁵, because there are many Ca^{2+} -binding proteins, which chelate free Ca^{2+} , in the cell. We have identified β subunit interacting proteins using yeast two-hybrid screening with a mouse brain complementary DNA library. One of the proteins is the Rab3-interacting molecule 1

(RIM1)¹⁶. *in vitro* pulldown assays using GST fusion constructs identified the RIM1 C terminus (residues 1079–1463) as a major β_4 subunit-interaction domain. Full-length RIM1 was coimmunoprecipitated with β_4 subunit of VDCC. Further we characterized the association between native VDCCs and RIM1 biochemically, using sucrose density gradient fractionation of neuronal VDCC complexes from mouse brains through microsome preparation. Western blot analysis of sucrose gradient fractions showed cosedimentation of RIM1 with Cav2.1 and β_4 subunit, but not from lethargic mice, which lack β_4 subunit.

The RIM1 was originally identified as a putative effector for the synaptic vesicle protein Rab3¹⁷, and comprises the RIM superfamily with other members that share C₂B domain at their C-termini¹⁸. RIM1 interacts with several other active zone protein components, including Munc13, ELKS/CAST, RIM-BP, or Liprins, to form a protein scaffold in the presynaptic nerve terminal¹⁹⁻²³. Mouse knockouts revealed that, in different types of synapses, RIM1 is essential for different forms of synaptic plasticity^{22, 24}. In the CA1-region Schaffer-collateral excitatory synapses and in GABAergic synapses, RIM1 is required for maintaining normal neurotransmit-

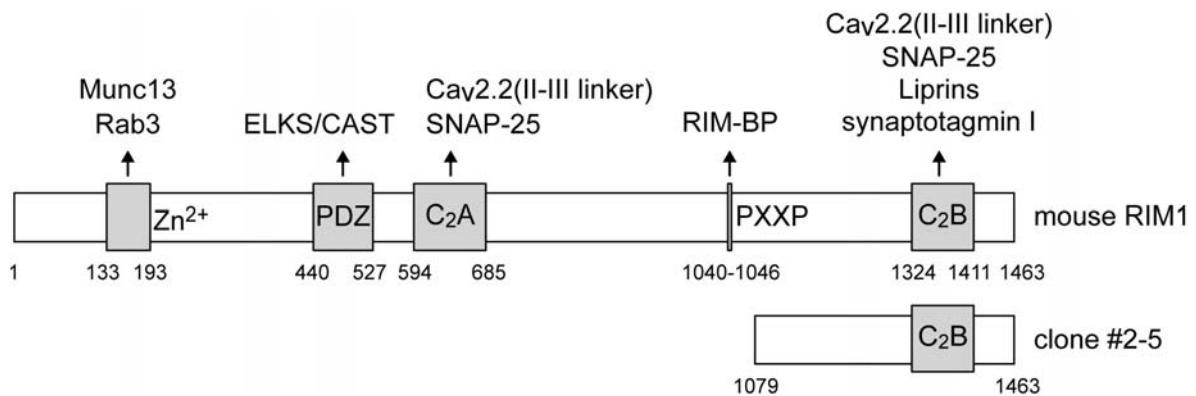


Figure 1 Domain structure of mouse RIM1.

Arrows indicate molecules interacting with RIM1 at the following domains: Zn^{2+} , Zn^{2+} -finger like domain; PDZ, PDZ domain; C₂A and C₂B, first and second C₂ domains; PXXP, proline-rich region. The protein region encoded by clone #2-5 is also indicated. "Adapted from reference 16 with permission"

ter release and short-term synaptic plasticity. In contrast, in excitatory CA3- region mossy fibre synapses and cerebellar parallel fibre synapses, RIM1 is necessary for presynaptic long-term, but not short-term, synaptic plasticity. In

autaptic neurons, the deletion of RIM1 causes a significant reduction in the readily releasable pool of vesicles, alters short-term plasticity, and changes the properties of evoked asynchronous release²⁵).

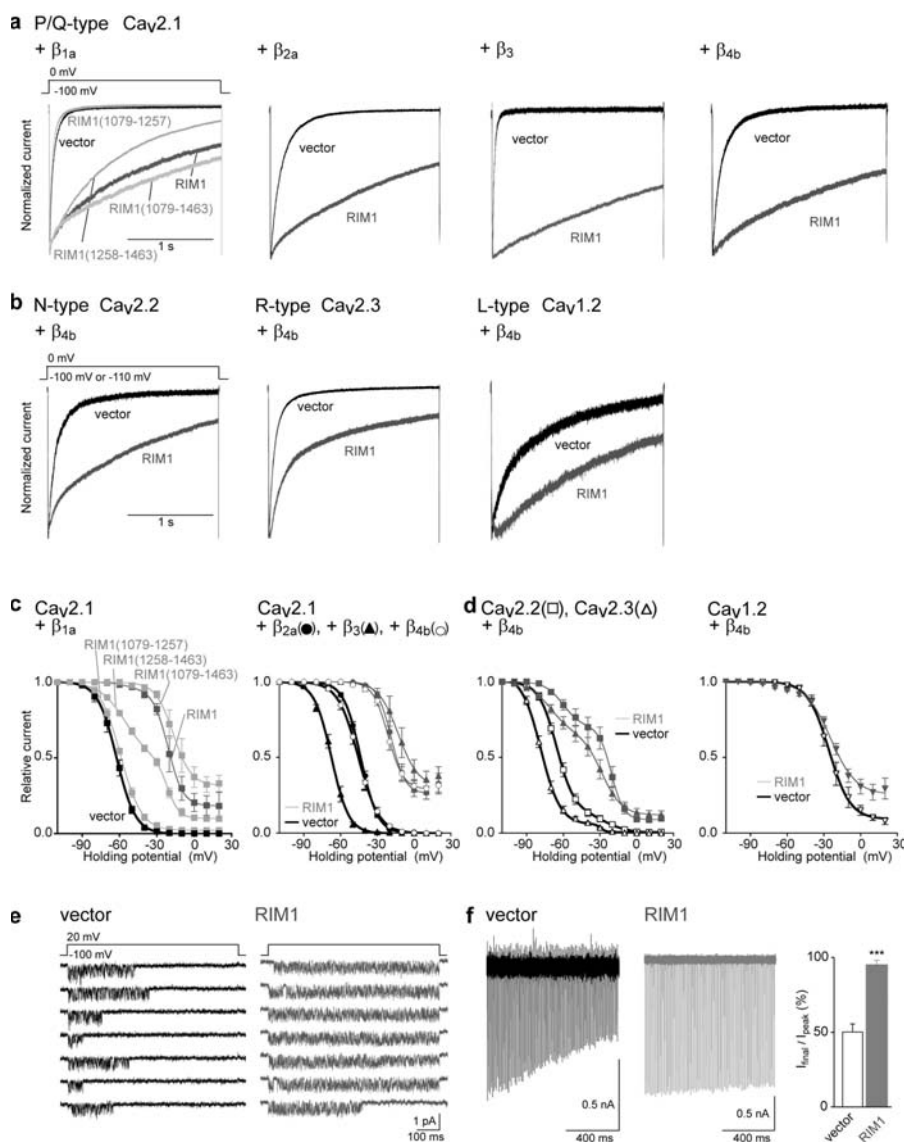


Figure 2 Effects of RIM1 on the inactivation properties of recombinant neuronal VDCCs.

(a) Inactivation of P/Q-type $Ca_v2.1$ currents in BHK cells expressing α_2/δ and β -subunits. For comparison of inactivation time courses after expression of RIM1 constructs, the peak amplitudes are normalized for Ba^{2+} currents elicited by 2-s pulses to 0 mV from a holding potential (V_h) of -100 mV. (b) Inactivation of N-type $Ca_v2.2$, R-type $Ca_v2.3$, or L-type $Ca_v1.2$ currents in BHK cells expressing α_2/δ and β_{4b} . The V_h is -100 mV for $Ca_v2.2$ or $Ca_v1.2$, and -110 mV for $Ca_v2.3$. (c) Left: inactivation curves for $Ca_v2.1$ in BHK cells expressing α_2/δ and β_{1a} . Right: inactivation curves for $Ca_v2.1$ in BHK cells expressing α_2/δ and different β -subunits. (d) Inactivation curves for $Ca_v2.2$, $Ca_v2.3$ (left), or $Ca_v1.2$ (right) in BHK cells expressing α_2/δ and β_{4b} . (e) RIM1 prolongs the time between first channel opening and last closing within a single-channel trace of $Ca_v2.1$ in BHK cells expressing α_2/δ and β_{4b} . Seven consecutive unitary traces are shown. The mean values for the time of each trace are 184.2 ± 33.3 ms ($n = 117$ traces) for vector and 502.8 ± 33.3 ms, ($n = 101$) for RIM1. The time for traces without opening is counted as 0 ms. (f) Left: $Ca_v2.1$ currents induced by 100 Hz AP trains for 1 s in BHK cells expressing α_2/δ and β_{1a} . Right: percentage of currents in response to the last stimulus compared to the peak current ($n = 6$ for vector and $n = 4$ for RIM1). Data points are mean \pm S.E.M. *** $P < 0.001$. "Adapted from reference 16 with permission"

Modulation of VDCCs inactivation by RIM1

To elucidate the functional significance of the direct RIM1- β_4 coupling, we characterized whole-cell Ba^{2+} currents through recombinant VDCCs expressed as $\alpha_1\alpha_2/\delta\beta$ complexes in baby hamster kidney (BHK) cells. RIM1 was tested with VDCC containing various neuronal α_1 -subunits, N-type $\text{Ca}_v2.2$, P/Q-type $\text{Ca}_v2.1$, R-type $\text{Ca}_v2.3$, and L-type $\text{Ca}_v1.2$. The most prominent effect of RIM1 on VDCC currents was observed on inactivation parameters. The rate of inactivation was dramatically decelerated (Fig. 2a,b). P/Q-type $\text{Ca}_v2.1$ channel currents in response to test pulse to 0 mV were inactivated within 500 ms in the absence of RIM1, however, less than 70% of the channels were inactivated even after the 2-s test pulse to 0 mV in the presence of RIM1. N-type $\text{Ca}_v2.2$, R-type $\text{Ca}_v2.3$, and L-type $\text{Ca}_v1.2$ VDCCs also inactivated slowly in the presence of RIM1 (Fig. 2b). RIM1 significantly shifted the inactivation curves (Fig. 2c,d), which is obtained by the double-pulse protocol. VDCC currents evoked by 20-ms test pulse to 0 mV after the 10-ms repolarization to -100 mV following 2-s holding potential displacement from -80 to 0 mV with 10-mV increments. In P/Q-types, RIM1 coexpression shifted the half inactivation potential by +24.6 mV and elicited an inactivation curve with a component susceptible to inactivation induced at high voltages ($V_{0.5} - \text{RIM1} = -45.9$ mV, $V_{0.5} + \text{RIM1} = -21.3$ mV; $V_{0.5}$ is the potential to give a half-value of inactivation) and a non-inactivating component. In N- and R-types, the major phase in biphasic inactivation curves was switched from low voltage-induced phases ($V_{0.5}$ and ratio; -64.5 mV and 0.91 for N, and -78.2 mV and 0.91 for R) to high voltage-induced phases ($V_{0.5}$ and ratio; -20.8 mV and 0.61 for N, and -27.9 mV and 0.53 for R). The non-inactivating component of the L-type inactivation curve was significantly

augmented by RIM1 (from 0.07 to 0.25). In P/Q-type channels, the effects on kinetics and voltage-dependent equilibrium of inactivation were elicited by RIM1 after replacement of β_{4b} with other β -subunits including β_{1a} , β_{2a} and β_3 , and as well by the C-terminal truncated mutants RIM1(1079-1463) and RIM1(1258-1463) but not by RIM1(1079-1257) (Fig. 2a,c). After RIM1 coexpression, single-channel currents clearly demonstrated prolongation of mean time between first channel opening and last closing within a trace during 750-ms depolarization to 20 mV without significant changes in single-channel amplitude (0.59 pA) (Fig. 2e). This observation corresponds well with the whole-cell data and suggests the predominant stabilization by RIM1 of the non-inactivating mode²⁶⁾ in P/Q-type channels. Instead of square test pulses, we used action potential waveforms, a more physiological voltage-clamp protocol to reveal closed-state inactivation²⁷⁾. action potentials began at -80 mV and peaked at 33 mV. Maximal rising and falling slopes were 300 V/s and -100 V/s, respectively. Currents evoked by the action potential waveforms further support the profound suppression of voltage-dependent inactivation by RIM1 (Fig. 2f). The observed effect of RIM1 on P/Q-type inactivation is attributable to its association with the β -subunits, since replacement of β_4 with its C-terminal truncation constructs, that directly act on α_1 ²⁸⁾ but cannot bind RIM1, failed to significantly affect inactivation in N-type channels. In support, BADN, the dominant negative form for the RIM1 action on VDCC β s, significantly diminished the effect of RIM1 on inactivation of P/Q channels. When Ca^{2+} was used (5 mM) as a physiological charge carrier in the experimental condition to induce Ca^{2+} -dependent inactivation²⁹⁾, RIM1 still exerted prominent suppressive effects on inactivation, slowing the speed and shifting the voltage dependence toward depolarizing potentials in

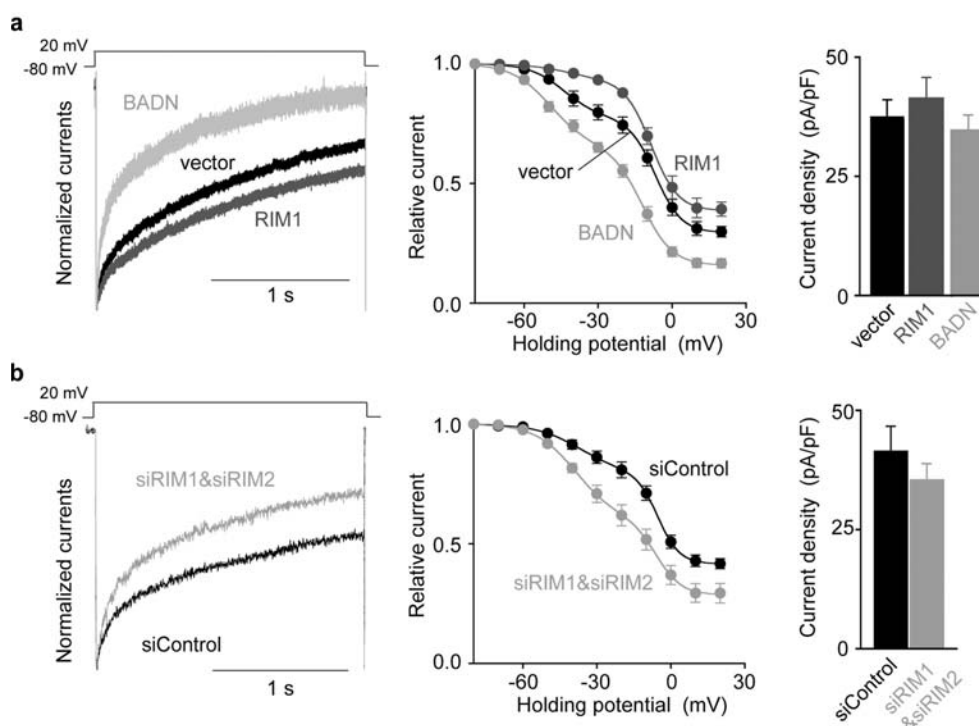


Figure 3 Physiological relevance of effects of RIM1 on inactivation properties of VDCCs.

(a) Effects of RIM1 and BADN on the inactivation properties of native VDCCs in PC12 cells maintained for 7-9 culture passages. Left: normalized currents recorded from PC12 cells transfected with vector, RIM1, and BADN. Middle: inactivation curves induced by 2-s holding potential displacement. Right: comparison of current densities at 10 mV ($n = 18, 15,$ and 9 cells for vector, RIM1, and BADN, respectively). (b) Acceleration of inactivation by coapplication of siRNAs specific for RIM1 and RIM2 (siRIM1 & siRIM2) in VDCC currents recorded from PC12 cells. PC12 cells were maintained for 2-3 culture passages. Left: normalized currents evoked by step pulses to 20 mV. Middle: inactivation curves induced by 2-s holding potential displacement. Right: comparison of current densities at 10 mV ($n = 6$ and 8 cells, for control GAPDH siRNA (siControl) and siRIM1 & siRIM2, respectively). Data points are mean \pm S.E.M. "Adapted from reference 16 with permission"

P/Q-type expressed in HEK cells (Fig 3a,b). Importantly, in rat pheochromocytoma PC12 neuroendocrine cells, BADN and co-application of siRNAs specific for RIM1 and RIM2 accelerated inactivation and shifted the inactivation curve for toward hyperpolarizing direction (Fig. 3c,d). This supports physiological significance of the effect of RIM1 via β on VDCC activation. Notably, as observed in RIM1-expressing cells, voltage-dependent inactivation of presynaptic VDCC currents at membrane potentials ≥ -40 mV was demonstrated in the previous report³⁰. Thus, RIM1 exerts strong effects on kinetics and voltage dependence of inactivation of N-, P/Q-, R- and L-types.

Many therapeutic drugs interact with voltage-gated channels. The molecular mechanisms of

drug actions are usually explained by the three main functional voltage-gated channel model, including resting (R), active or open (O), and inactivated (I) states¹. In this context, the RIM1 effects can be explained by the three-states-model. In the absence of RIM1, channels go into inactivation state through open state at a membrane potential of 0 mV. On the other hand, in the presence of RIM1, channels stay open state preferentially, and then move into inactivation state slowly. At -50 mV, 80% of the channels are inactivated in the absence of RIM1, however, in the presence of RIM1 almost all channels stay resting state. Because -50 mV is subthreshold voltage, at -50 mV, resting state channels move into inactivation state directly in the absence of RIM1. RIM1 removes the direct

route from the resting state to the inactivation state.

P-type current was first identified in cerebellar Purkinje cells and is characterized by very slow inactivation kinetics^{31,32}. Thereafter, Q-type current was identified in cerebellar granule cells and is characterized by fast inactivation kinetics³². Although P- and Q-type VDCCs show distinct properties, knock-out studies clearly demonstrated that both of them are coded by the same $Ca_v2.1$ ^{33,34}. Human $Ca_v2.1$ did not produce the P-type current but produced the Q-type current, when expressed in human embryonic kidney cells³⁵. However, the P-type current was recorded in the knock-in mice which express the human $Ca_v2.1$ instead of mouse $Ca_v2.1$ ³⁶. These results suggested that some additional factors, such as post-translational processing or interaction with other proteins, may be necessary to produce the P-type current. One of the candidates to change the channel types is RIM1.

In terms of RIM1 effects on other functional parameters such as voltage dependence of activation, activation kinetics, and current densities at different voltages in current-voltage relationships, VDCCs can be categorized into two different groups. In β_{4b} -expressing BHK cells, the current densities of the N- and P/Q-type were significantly augmented by RIM1, while those of the R- and L-type ($Ca_v1.2$) were unaffected by RIM1. In P/Q-type, the C-terminal region (1079-1463), that carries the β association site, was sufficient for the RIM1 action to enhance the current density. By contrast, activation speeds were significantly decelerated and activation curves were shifted toward positive potentials by RIM1 in R- and L-type, but not in N- and P/Q-type. When β_{4b} was replaced with other β -isoforms, the augmentation of P/Q-type current densities by RIM1 was abolished, whereas the effect by RIM1 on activation speed of P/Q-type was induced

by the β -subunits other than β_{4b} ; activation was decelerated in the presence of β_{1a} , β_{2a} , and β_3 (Fig. 3d, right panel). The RIM1 effect shifting activation curve toward positive potentials was also elicited by β_{2a} in P/Q-type. Thus, the group comprised of the N- and P/Q-type and the group comprised of the R- and L-type ($Ca_v1.2$) behave contrastively with regard to sensitivity to RIM1 in activation kinetics, voltage dependence of activation, and current densities.

A synapse-localized E3 ubiquitin ligase, SCRAPPER, regulates neural transmission. SCRAPPER directly binds, ubiquitinates and degrades RIM1. In neurons from Scrapper-knockout (SCR-KO) mice, RIM1 had a longer half-life with significant reduction in ubiquitination. As a result of the RIM1 degradation defect, SCR-KO mice displayed altered electrophysiological synaptic activity, i.e., increased frequency of miniature excitatory postsynaptic currents³⁷. This phenotype of SCR-KO mice is similar to RIM1 overexpression.

Enhancement of neurotransmitter release by the association of VDCC β subunit with RIM1

To gain insight into the physiological relevance of the RIM1 interaction with the VDCC complex, we assessed neurotransmitter release from PC12 cells in which diverse high voltage-activated types of VDCCs were characterized in detail^{26,38}. PC12 cells were transfected with RIM1 construct cDNAs along with the choline acetyltransferase (ChAT) gene that synthesizes ACh for synaptic vesicles³⁹. The ACh release triggered by a Ca^{2+} influx in response to membrane depolarization via high K^+ stimulation (elevation of extracellular K^+ concentration from 4.7 mM to 49.9 mM) was significantly potentiated by full-length RIM1. ACh release was also enhanced by the Rab3-interacting N-terminal Zn^{2+} finger RIM1 subfragment (11-399) or by the C-terminal

β -interacting RIM1 domain (1079-1463) that maintains VDCC currents, but not by the middle subfragment RIM1(400-1078). In PC12 cells, BADN significantly suppressed ACh release, in sharp contrast with the full-length RIM1. In cultured cerebellar neurons, similar suppression by BADN and potentiation by the full-length RIM1 were observed for glutamate release upon high K^+ stimulation. The results suggest that RIM1 can potentiate neurotransmitter release through its interaction with VDCC β in PC12 cells.

Cone-rod dystrophy **CORD7**

A mutation has been identified for an autosomal dominant cone-rod dystrophy **CORD7** in the *RIMI* gene that is localized to chromosome 6q14⁴⁰. A four-generation British family with **CORD7** first experienced reduced color vision and visual acuity between the ages of 20 and 40 years. As the disorder progressed, they had difficulty seeing in bright light, and one individual reported visual problems in dim light. At the onset of symptoms, retinal pigmentary changes were already present around the fovea, simulating bull's eye dystrophy, which developed into macular atrophy⁴¹. Interestingly, the affected individuals also showed significantly enhanced cognitive abilities across a range of domains⁴². Thus, the **CORD7** RIM1 mutation is characterized by retinal dystrophy and enhanced brain function. To elucidate the mechanisms underlying these phenotypes, a nucleotide (G to A) substitution, that replaces Arg-655 with His in the middle C2A domain reported for its ability to bind to VDCC α_1 -subunit²⁴, was introduced in the mouse RIM1 cDNA to yield a construct which carries a mutation corresponding to human **CORD7** RIM1 mutation R844H⁴⁰. The mouse clone differs from the human clone in having a deletion in the region between the Zn^{2+} -finger-like and PDZ domains. In this region, no specific

functional domains have yet been identified. Co-immunoprecipitation experiments suggested an intact interaction between RIM1 mutant R655H and the VDCC β_{4b} -subunit. To elucidate the functional effects of the RIM1 mutant, we characterized whole-cell Ba^{2+} currents through recombinant VDCCs expressed as $\alpha_1\alpha_2/\delta\beta_{4b}$ complexes containing neuronal α_1 -subunits Cav2.1 of P/Q-type VDCCs or Cav1.4 of L-type VDCCs. These VDCCs were selected, because P/Q-type Cav2.1 plays an important role in neurotransmitter release from central neurons², while L-type Cav1.4 is found at high densities in photoreceptor terminals^{43,44} and is known for its association with X-linked congenital stationary night blindness⁴⁵. When compared to wild-type RIM1 (WT), R655H significantly increased the non-inactivating component of P/Q-type Cav2.1 currents (from 0.30 ± 0.04 (n = 6) to 0.43 ± 0.03 (n = 9); $p < 0.01$). Inactivation parameters of L-type Cav1.4 currents were unaffected by R655H RIM1. In terms of activation properties, the voltage dependence of P/Q-type (Cav2.1) current activation was shifted toward negative potentials and activation speed was increased by R655H expression. Furthermore, RIM1-mediated augmentation of Cav2.1 current density was significantly enhanced by R655H. In contrast to Cav2.1 currents, the RIM1-mediated hyperpolarizing shift of Cav1.4 activation was abolished by the mutation. The effects of R655H on activation speed and current density were indistinguishable from those of WT RIM1 for Cav1.4 channels.

The mouse RIM1 mutant R655H, equivalent to the human **CORD7** mutation, alters RIM1 function in regulating VDCC currents. For P/Q-type Cav2.1 VDCC, important in neurotransmitter release at central synapses, the **CORD7** mutation accelerated activation, and enhanced the RIM1-mediated suppression of inactivation and augmentation of current density, likely leading to enhanced neurotransmitter release

and synaptic transmission. In contrast, for L-type Cav1.4 VDCC, a predominant player in glutamate release from photoreceptor terminals, the CORD7 mutation abolished the RIM1-mediated hyperpolarization of current activation, likely resulting in impaired synaptic transmission at ribbon synapses of the visual system. The variable effects of this CORD7 mutation on different presynaptic VDCCs may underlie the two reported nervous system phenotypes, retinal dystrophy and enhanced cognitive abilities.

References

- 1) Hille B. *Ionic Channels of Excitable Membranes*, 3rd Ed, 2001; Sinauer Associates, Sunderland, MA.
- 2) Tsien RW, Ellinor PT, Horne WA. Molecular diversity of voltage-dependent Ca²⁺ channels. *Trends Pharmacol Sci* 1991;12:349-54.
- 3) Catterall WA. Structure and function of neuronal Ca²⁺ channels and their role in neurotransmitter release. *Cell Calcium* 1998;24:307-23.
- 4) Takahashi T, Momiyama A. Different types of calcium channels mediate central synaptic transmission. *Nature* 1993;366:156-8.
- 5) Wheeler DB, Randall A, Tsien RW. Roles of N-type and Q-type Ca²⁺ channels in supporting hippocampal synaptic transmission. *Science* 1994; 264:107-11.
- 6) Ertel EA, Campbell KP, Harpold MM, Hofmann F, Mori Y, Perez-Reyes E, et al. Nomenclature of voltage-gated calcium channels. *Neuron* 2000; 25:533-5.
- 7) Bichet D, Cornet V, Geib S, Carlier E, Volsen S, Hoshi T, et al. The I-II loop of the Ca²⁺ channel α_1 subunit contains an endoplasmic reticulum retention signal antagonized by the beta subunit. *Neuron* 2000;25:177-90.
- 8) Mori Y, Friedrich T, Kim MS, Mikami A, Nakai J, Ruth P, et al. Primary structure and functional expression from complementary DNA of a brain calcium channel. *Nature* 1991;350:398-402.
- 9) Schultz D, Mikala G, Yatani A, Engle D B, Iles D E, Segers B, et al. Cloning, chromosomal localization, and functional expression of the α_1 subunit of the L-type voltage-dependent calcium channel from normal human heart. *Proc Natl Acad Sci USA* 1993;90:6228-32.
- 10) Wakamori M, Mikala G, Schwartz A, Yatani A. Single-channel analysis of a cloned human heart L-type Ca²⁺ channel α_1 subunit and the effects of a cardiac β subunit. *Biochem Biophys Res Commun* 1993;196:1170-76.
- 11) Wakamori M, Niidome T, Furutama D, Furuichi T, Mikoshiba K, Fujita Y, et al. Distinctive functional properties of the neuronal BII (class E) calcium channel. *Receptors Channels* 1994;2:303-14.
- 12) Wakamori M, Mikala G, Mori Y. Auxiliary subunits operate as a molecular switch in determining gating behaviour of the unitary N-type Ca²⁺ channel current in *Xenopus* oocytes. 1999; 517:659-72.
- 13) Zhai RG, Bellen HJ. The architecture of the active zone in the presynaptic nerve terminal. *Physiology (Bethesda)* 2004;19:262-70.
- 14) Atwood HL. Neuroscience. Gatekeeper at the synapse. *Science* 2006;312:1008-9.
- 15) Neher E. Vesicle pools and Ca²⁺ microdomains: new tools for understanding their roles in neurotransmitter release. *Neuron* 1998;20:389-99.
- 16) Kiyonaka S, Wakamori M, Miki T, Urie Y, Nonaka M, Bito H, et al. RIM1 confers sustained activity and neurotransmitter vesicle anchoring to presynaptic Ca²⁺ channels. *Nat Neurosci* 2007; 10:691-701.
- 17) Wang Y, Okamoto M, Schmitz F, Hofmann K, Sudhof TC. Rim is a putative Rab3 effector in regulating synaptic-vesicle fusion. *Nature* 1997; 388:593-8.
- 18) Wang Y, Sudhof TC. Genomic definition of RIM proteins: evolutionary amplification of a family of synaptic regulatory proteins (small star, filled). *Genomics* 2003;81:126-37.
- 19) Wang Y, Sugita S, Sudhof TC. The RIM/NIM family of neuronal C2 domain proteins. Interactions with Rab3 and a new class of Src homology 3 domain proteins. *J Biol Chem* 2000; 275:20033-44.

- 20) Betz A, Thakur P, Junge HJ, Ashery U, Rhee JS, Scheuss V, et al. Functional interaction of the active zone proteins Munc13-1 and RIM1 in synaptic vesicle priming. *Neuron* 2001;30:183-96.
- 21) Ohtsuka T, Takao-Rikitsu E, Inoue E, Inoue M, Takeuchi M, Matsubara K, et al. Cast: a novel protein of the cytomatrix at the active zone of synapses that forms a ternary complex with RIM1 and munc13-1. *J Cell Biol* 2002;158:577-90.
- 22) Schoch S, Castillo PE, Jo T, Mukherjee K, Geppert M, Wang Y, et al. RIM1alpha forms a protein scaffold for regulating neurotransmitter release at the active zone. *Nature* 2002;415:321-6.
- 23) Coppola T, Magnin-Luthi S, Perret-Menoud V, Gattesco S, Schiavo G, Regazzi R. Direct interaction of the Rab3 effector RIM with Ca^{2+} channels, SNAP-25, and synaptotagmin. *J Biol Chem* 2001;276:32756-62.
- 24) Castillo PE, Schoch S, Schmitz F, Sudhof TC, Malenka RC. RIM1alpha is required for presynaptic long-term potentiation. *Nature* 2002;415:327-30.
- 25) Calakos N, Schoch S, Sudhof TC, Malenka RC. Multiple roles for the active zone protein RIM1alpha in late stages of neurotransmitter release. *Neuron* 2004;42:889-96.
- 26) Plummer MR, Logothetis DE, Hess P. Elementary properties and pharmacological sensitivities of calcium channels in mammalian peripheral neurons. *Neuron* 1989;2:1453-63.
- 27) Patil PG, Brody DL, Yue DT. Preferential closed-state inactivation of neuronal calcium channels. *Neuron* 1998;20:1027-38.
- 28) De Waard M, Pragnell M, Campbell KP. Ca^{2+} channel regulation by a conserved β subunit domain. *Neuron* 1994;13:495-503.
- 29) DeMaria CD, Soong TW, Alseikhan BA, Alvania RS, Yue DT. Calmodulin bifurcates the local Ca^{2+} signal that modulates P/Q-type Ca^{2+} channels. *Nature* 2001;411:484-9.
- 30) Stanley EF. Syntaxin I modulation of presynaptic calcium channel inactivation revealed by botulinum toxin C1. *Eur J Neurosci* 2003;17:1303-5.
- 31) Llinas R, Sugimori M, Lin JW, Cherksey B. Blocking and isolation of a calcium channel from neurons in mammals and cephalopods utilizing a toxin fraction (FTX) from funnel-web spider poison. *Proc Natl Acad Sci USA* 1989;86:1689-93.
- 32) Randall A, Tsien RW. Pharmacological dissection of multiple types of Ca^{2+} channel currents in rat cerebellar granule neurons. *J Neurosci* 1995;15:2995-3012.
- 33) Jun K, Piedras-Renteria ES, Smith SM, Wheeler DB, Lee SB, Lee TG, et al. Ablation of P/Q-type Ca^{2+} channel currents, altered synaptic transmission, and progressive ataxia in mice lacking the α_{1A} - subunit. *Proc Natl Acad Sci USA* 1999;96:15245-50.
- 34) Fletcher CF, Tottene A, Lennon VA, Wilson SM, Dubel SJ, Paylor R, et al. Dystonia and cerebellar atrophy in *Cacna1a* null mice lacking P/Q calcium channel activity. *Faseb J* 2001;15:1288-90.
- 35) Toru S, Murakoshi T, Ishikawa K, Saegusa H, Fujigasaki H, Uchihara T, et al. Spinocerebellar ataxia type 6 mutation alters P-type calcium channel function. *J Biol Chem* 2000;275:10893-8.
- 36) Saegusa H, Wakamori M, Matsuda Y, Wang J, Mori Y, Zong S, et al. Properties of human Cav2.1 channel with a spinocerebellar ataxia type 6 mutation expressed in Purkinje cells. *Mol Cell Neurosci* 2007;34:261-70.
- 37) Yao I, Takagi H, Ageta H, Kahyo T, Sato S, Hatanaka K, et al. SCRAPER-dependent ubiquitination of active zone protein RIM1 regulates synaptic vesicle release. *Cell* 2007;130:943-57.
- 38) Liu H, Felix R, Gurnett CA, De Waard M, Witcher DR, Campbell KP. Expression and subunit interaction of voltage-dependent Ca^{2+} channels in PC12 cells. *J Neurosci* 1996;16:7557-65.
- 39) Nishiki T, Shoji-Kasai Y, Sekiguchi M, Iwasaki S, Kumakura K, Takahashi M. Comparison of exocytotic mechanisms between acetylcholine- and catecholamine-containing vesicles in rat pheochromocytoma cells. *Biochem Biophys Res Commun* 1997;239:57-62.
- 40) Johnson S, Halford S, Morris AG, Patel RJ, Wilkie SE, Hardcastle AJ, et al. Genomic organisation and alternative splicing of human RIM1, a gene

- implicated in autosomal dominant cone-rod dystrophy (CORD7). *Genomics* 2003;81:304-14.
- 41) Kelsell RE, Gregory-Evans K, Gregory-Evans CY, Holder GE, Jay MR, Weber BH, et al. Localization of a gene (CORD7) for a dominant cone-rod dystrophy to chromosome 6q. *Am J Hum Genet* 1998;63:274-9.
- 42) Sisodiya SM, Thompson PJ, Need A, Harris SE, Weale ME, Wilkie SE, et al. Genetic enhancement of cognition in a kindred with cone-rod dystrophy due to RIMS1 mutation. *J Med Genet* 2007;44:373-80.
- 43) Koschak A, Reimer D, Walter D, Hoda JC, Heinzle T, Grabner M, et al. Cav1.4 α 1 subunits can form slowly inactivating dihydropyridine-sensitive L-type Ca²⁺ channels lacking Ca²⁺-dependent inactivation. *J Neurosci* 2003;23:6041-9.
- 44) McRory JE, Hamid J, Doering CJ, Garcia E, Parker R, Hamming K, et al. The CACNA1F gene encodes an L-type calcium channel with unique biophysical properties and tissue distribution. *J Neurosci* 2004;24:1707-18.
- 45) Bech-Hansen NT, Naylor MJ, Maybaum TA, Pearce WG, Koop B, Fishman GA, et al. Loss-of-function mutations in a calcium-channel α 1-subunit gene in Xp11;23 cause incomplete X-linked congenital stationary night blindness. *Nat Genet* 1998;19:264-7.